Fast picomolar selective detection of bisphenol A in water using a carbon nanotube field effect transistor functionalized with estrogen receptor-α

Zayda C. Sánchez-Acevedo[+], Jordi Riu* and F. Xavier Rius
Department of Analytical and Organic Chemistry, University Rovira i Virgili,
43007 Tarragona, Spain

11 Pages
5 Figures

*Please address correspondence to:

Jordi Riu
Department of Analytical and Organic Chemistry
Universitat Rovira i Virgili
Campus Sescelades
C/ Marcel·lí Domingo s/n
43007 – Tarragona
Catalonia – Spain

Tel.: +34 977 558 491
Fax.: +34 977 558 446
e-mail: jordi.riu@urv.cat

[+] ZC Sánchez-Acevedo is on leave from the University of Pamplona (Colombia)

Abstract

In this paper we report a biosensor for the fast, ultrasensitive and selective determination of bisphenol A in water. It is based on a field effect transistor (FET) in which a network of single-walled carbon nanotubes (SWCNTs) acts as the conductor channel. SWCNTs are functionalized for the first time with a nuclear receptor, the estrogen receptor alpha (ER-α), which is adsorbed onto the SWCNTs and acts as the sensing part of the biosensor. SWCTNs are subsequently protected to prevent the non-specific binding of interferences. With this biosensor we can detect picomolar concentrations of BPA in only two minutes of analysis. Selectivity has been tested against possible interferences such as fluoranthene, pentacloronitrobenzene and malathion, and this is the first device that experimentally shows that small molecules can also be selectively detected at ultralow concentrations using a CNTFET biosensor.

Keywords: carbon nanotubes, nuclear receptor, BPA, nanotechnology; picomolar detection

1. Introduction

Nowadays, due to the fabrication of a large variety and quantity of chemical products, xenobiotic compounds can be found in the human organism, even though they should be absent from them. Some of these xenocompounds, called xenoestrogens, have a similar structure to estrogens and hence exhibit an affinity for the human estrogen receptor (ER). ER is a member of the nuclear receptor family and can exist in two species, ER-α and ER-β, with different tissue distribution (Hiroi et al., 1999). The similarity between xenoestrogens and estrogens is the main reason for the increase of a series of diseases and the appearance of others related to the estrous cycle, among which we can identify masculine infertility, functional alterations of sexual development and an increase in some types of cancer (Oosterkamp et al. 1997; Mueller, 2004). Among xenoestrogens, bisphenol A (BPA), which is widely used as a primary monomer in plastics or resins, as an antioxidant in plasticizers and as a polymerization inhibitor in PVC (polyvinyl chloride), has been shown to possess strong estrogenic properties and exhibits both agonistic and antagonistic actions for ER-α while only exhibits agonistic actions for ER-β.

Although the current BPA US-EPA reference dose for humans is 50 μg $kg^{-1}day^{-1}$, research shows that recently discovered estrogen receptors associated with the cell

membrane can stimulate physiological responses at BPA concentrations of picograms per ml (ppt) (Walsh et al., 2005; Wozniak et al., 2005; Zsarnovszky et al., 2005). This makes BPA equipotent to 17β-estradiol (Hiroi et al., 1999; Vom Saal et al., 2007). Xenoestrogenic compounds can be detected and quantified using a wide variety of analytical techniques. Amongst them, chromatographic techniques are undoubtedly the most commonly used and combined with different detection methods (Moors et al. 2007; Inoue et al., 2006; Peng et al., 2006). However, the methodologies employed so far require complex equipment. Also, pretreatment stages such as pre-concentration and other sample treatments are time-demanding and labour intensive (Kawaguchi et al., 2004; Gatidou et al, 2007; Hu et al., 2007). Recent detection methods of BPA in water include, among others, the use of antibodies in a yeast two-hybrid bioassay (Schwartz-Mittelman et al., 2005) with a limit of detection of $1.75x10^{-9}$ M in 6 minutes of measurement, potentiometric methods with response times of 5 minutes and a limit of detection of $2.63x10^{-9}$ M (Piao et al., 2008) or optical immunosensors with an analysis time per sample of 15 minutes and a limit of detection of $6.13x10^{-11}$ M. (Rodríguez-Mozaz et al., 2005)

New types of sensors have been developed in recent years with the emergence of nanostructured materials. The nanometric size related to these new materials (usually less than 100 nm in at least one dimension) is important for revealing new properties which are different from those exhibited by the same materials in bulk size. Sensors incorporating nanoparticles, carbon nanotubes or cantilevers (among other nanostructures), potentially display several advantageous performance characteristics such as increased sensitivity, improved detection limits, faster instrumental responses or the use of smaller amounts of test samples (Riu et al., 2007). A group of these new nanomaterials is formed by the carbon nanotubes (CNTs) discovered by S. Iijima in 1991 (Iijima, 1991). One specific type of electrochemical CNT sensor is the so called carbon nanotube field-effect transistor (CNTFET), built using single-walled carbon nanotubes (SWCNT). (Star et al., 2003; Star et al., 2004) One of the main advantages of these CNTFET is their high sensitivity, attributed to the outstanding capacity of SWCNTs to promote electron transfer between heterogeneous phases. (Chen et al, 2003) Nevertheless, SWCNTs sensitivity to the presence of different molecules in their surrounding chemical environment is also a drawback due to interference from these molecules or their influence on selectivity. Since carbon nanotubes are sensitive to many substances, it is necessary to protect and functionalize SWCNTs to become selective to the selected target molecule. The CNFET developed so far (Grüner, 2006; Kauffman and Star, 2008; Kim et al., 2007) have been mostly devoted to detecting

large compounds such as proteins, (Star et al., 2003; Shim et al., 2002; Byon and Choi, 2006) DNA sequences, (Star et al, 2006) immunoglobulins (Chen et al., 2003; Maehashi et al., 2007; Cid et al., 2008) or bacteria. (Villamizar et al., 2008; So et al., 2008) Recently Zhao et al. (Zhao et al., 2008) developed a CNTFET functionalized with a small synthetic receptor, pyrenecyclodextrin, that was able to detect a range of small chemicals, although no experimental influence from any other compounds was reported in this paper. Therefore, interferences and selectivity still need to be checked from a practical point of view for the selective detection of small compounds using CNTFET devices. Silicon nanowires field-effect transistors, which are closely related to CNTFET devices, have been also successfully used for detecting small molecules such as calcium ions (Bi et al., 2008) or dopamine (Lin et al., 2008).

In this paper we are reporting a CNTFET functionalized for the first time with a nuclear receptor, the human estrogen receptor α (ER-α), which allows the selective detection of picomolar concentrations of bisphenol A (BPA) in water. In this way we are showing for the first time that CNTFETs functionalized with large compounds can successfully detect small molecules at ultralow concentrations checking the selectivity from a practical point of view. The recognition layer of this sensor is the ER-α. We therefore take advantage of the molecular recognition principles while trying, at the same time, to mimic nature. The ER-α is adsorbed onto the surface of a network of SWCNTs which act as transducers. A PBSTG solution (Piao et al., 2008) (0.05% Tween 20 and 0.8% gelatin in phosphate buffered saline, PBS) has been used as a blocking agent in order to avoid nonspecific adsorption of interferences over the SWCNTs. With this sensor we are able to detect 2.19×10^{-12} M of BPA in aqueous solution. This is the lowest concentration of BPA reported in the literature and was detected in only 2 minutes of analysis. The presence of interferences that can also be found in water samples like fluoranthene, pentacloronitrobenzene and malathion do not produce any electrical response to our biosensing device.

2. Experimental

2.1 Materials

The ER-α was purchased from Invitrogen Ltd (Paisley, UK). Milli-Q water/deionized and charcoal-treated water, 18.2 MΩ.cm specific resistance, was obtained with a Milli-Q Plus reagent-grade water system (Millipore, Billerica, MA). Sigma-Aldrich (Tres Cantos,

Spain) supplied the remaining reagents: Tween 20, gelatin from cold water fish skin, Dulbecco's PBS (phosphate buffered saline, 15 mM, pH=7.4), BPA, fluoranthene, pentachloronitrobenzene, malathion, isopropanol and iron (III) nitrate nonahydrate.

2.3 Apparatus

Environmental scanning electron microscopy (ESEM) FEI Quanta model 600 was used to obtain the images of the networks of SWCNTs. Electrical measurements were made using a 4157A Agilent semiconductor parameter analyzer and a Wentworth Laboratories MP1008 probe station.

2.3 Development of the CNTFETs

The network of SWCNTs was synthesized by chemical vapour deposition (CVD) on top of a layer of silicon dioxide (500 nm thickness) thermally grown on heavily n-type-doped silicon substrates. A solution of 100 mgL^{-1} of iron nitrate in isopropanol was deposited by spin coating over the SiO_2 layer as a catalyst for synthesis. CVD was performed at 900 ºC for 20 min with 600 sccm of methane and 200 sccm of hydrogen. About 70% of synthesised SWCNTs are semiconductor and the rest are metallic (Kim et al., 2002), which means that overall the network's behaviour is semiconducting. The National Microelectronics Centre CNM/CSIC (Bellaterra, Spain) then deposited source and drain electrodes of chromium/gold (2/30 nm thick, respectively) over the substrate containing the SWCNTs using photolithography and leaving a distance of 2.5 μm between them. The gate electrode was a layer of aluminium covering the back side of the Si substrate. Control experiments were conducted to show that there was no electrical current between the source and drain electrodes when only the particles of iron from the catalyst were deposited over the SiO_2 substrate (i.e. just before the CVD). AFM images show that the particles of iron are scattered over the SiO_2 substrate without forming a layer.

2.4 Functionalization of the CNTFETs

The CNTFETs were functionalized as follows. ER-α, the recognition molecule, is immobilized over the surface of the SWCNTs by immersing the devices overnight in a 10 mg L^{-1} solution of ER-α in PBS. After adsorbing the ER-α, the devices were rinsed with Milli-Q water, dried with nitrogen and immersed for three hours at room temperature in a PBSTG solution (0.05% Tween 20 and 0.8% gelatin in PBS). The

CNTFETs were again thoroughly rinsed with Milli-Q water, dried with nitrogen and electrically characterized by measuring three replicates and by plotting the mean value of these measurements. The CNTFETs were then ready to be used to detect BPA. Fig. 1 shows a scheme of the functionalization process

2.5 Detection of BPA

In order to avoid the ionic strength of the samples containing BPA, all the measurements were performed in dry conditions. The functionalized CNTFETs were exposed to increasing concentrations of BPA (from $2.19x10^{-12}$ M to $4.38\ x10^{-4}$ M of BPA; all the solutions were prepared in 10% PBS in milli-Q water). For each concentration, the CNTFETs were immersed for 2 minutes at room temperature in the corresponding solution of BPA. Then they were rinsed thoroughly with milli-Q water and dried with nitrogen. Three replicates of each sample containing BPA were also measured.

2.6 Selectivity of the CNTFETs

Selectivity was checked in the presence of three interferences: fluoranthene, pentacloronitrobenzene and malathion. A functionalized CNTFET was immersed for two minutes at room temperature in the solution of the corresponding interference. Then it was rinsed thoroughly with milli-Q water, dried with nitrogen and electrically characterized by measuring three replicates and by plotting the mean value of these measurements. The concentrations tested are from $4.95x10^{-12}$ M up to $4.95\ x10^{-5}$ M for fluoranthene, from $3.39x10^{-12}$ M up to $3.39\ x10^{-5}$ M for pentachloronitrobenzene and from $3.03x10^{-12}$ M up to $3.03\ x10^{-5}$ M for malathion.

3. Results and discussion

Fig. 2 shows an environmental scanning electron microscopy (ESEM) image of the source and drain electrodes and of the network of SWCNTs. The average height of the SWCNTs is estimated to be ca. 1.4 nm from atomic force microscope (AFM) measurements. The average height of the functionalized SWCNTs is ca. 9.3 nm. The density of the network was estimated to be around 1.5 nanotubes/μm^2, just above the percolation threshold, (Hu et al., 2004) to avoid a high number of conduction paths through metallic SWCNTs. This latter situation would lead to a reduction in the on/off ratio of the CNTFET and hence a reduction in the sensitivity of the sensing device.

Several papers in the literature claim that proteins are strongly and non-specifically adsorbed onto carbon nanotubes. (Star et al., 2003; Chen et al., 2003) The strong adsorption can be due to the hydrophobic interactions between the functional groups of the protein and the nanotube surface. (Chen et al., 2004; Bradley et al., 2004)

Fig. 3 shows the electrical characterization of the CNTFET during the different functionalization steps. All the measurements were made at room temperature in dry conditions by measuring three times the dependence of the source-drain current, I, with a constant bias voltage (Vsd) of 0.25 V, sweeping the back gate voltage, Vg, in the range of +5 V to -5 V. Each curve in Fig. 3 corresponds to the mean value of the three replicates. After adsorbing the ER-α over the SWCNTs there is a decrease in the electrical current through the CNTFET channel. These changes have been shown to be independent of the net charge of the adsorbed protein. The fact that the curve corresponding to the adsorption of ER-α in Fig. 3 is shifted toward more negative gate voltages seems to indicate that this decrease can be due to a charge transference (Heller et al., 2008) caused by a release of the electrons of the ER-α's amine groups (i.e. arginine and lysine residues) to the SWCNTs (Bradley et al., 2004; Chen et al., 2004). However, the change observed may also be due to a scattering potential effect originated by the adsorption of ER-α which decreases the mobility of holes in SWCNTs. (Star et al., 2003) The electrical current of the CNTFET also decreased after the adsorption of PBSTG. Fig. 3 shows that when a small concentration of 2.19×10^{-12} M of BPA is added to the functionalized CNTFET there is a change in the electrical conductivity, which shows the interaction between BPA and the functionalized CNTFET.

The response time of the interaction between ER-α and BPA was monitored to determine the analysis time of the CNTFET. The CNTFET functionalized device was exposed to a 4.38×10^{-11} M solution of BPA for different times (from 0.5 minutes to 5 minutes) and we recorded the electrical responses. We found that 0.5 minutes is enough for the interaction between ER-α and BPA to take place, because increasing this time (up to 5 minutes) does not significantly change the electrical response. Although the response time is 0.5 minutes, we decided to work with 2 minutes in order to be sure that the recognition process was completely fulfilled.

Control experiments were conducted to demonstrate that CNTFET devices functionalized without ER-α did not show any response in the presence of BPA. In order to check that the electrical response provided by the CNTFETs was given by the

specific interaction between ER-α and BPA and not because of the non-specific adsorption of interferences over the SWCNTs, a control blank experiment was conducted. A CNTFET without ER-α adsorbed over the SWCNTs was immersed for 3 h in a solution of PBSTG. The CNTFET was washed with milli-Q water and dried with nitrogen for subsequent electrical characterization. The exposure of this CNTFET device to a blank solution containing only PBS and to a four different concentrations of BPA ranging from 4.38×10^{-12} M to 4.38×10^{-6} M gave the same electrical curves (not shown) as the CNTFET device coated with the PBSTG solution. This shows that the PBSTG solution effectively coats the SWCNTs, and if there is a variation in the electrical signal, it is because the interaction between ER-α and BPA. In this way we proved that PBSTG was effectively protecting the SWCNTs against non-specific binding and that the decrease in the electrical current shown in Fig. 3 when adding BPA was only due to the interaction between ER-α and BPA.

Fig. 4a shows the electrical current of the functionalized CNTFET before (the PBSTG curve) and after exposure to different solutions from 2.19×10^{-12} M to 4.38×10^{-4} M of BPA. Fig. 4b shows that the presence of BPA significantly decreases the electrical current at negative gate voltages and shows that the interaction of ER-α with BPA significantly decreases the electrical current up to approximately 4.38×10^{-7} M of BPA (i.e. a decrease from 5.23% for 2.19×10^{-12} M of BPA to 67.94% for 4.38×10^{-7} M of BPA). From this latter concentration the signal tends to stabilize possibly due to the saturation of the ER-α. The highest relative standard deviation from the three replicates at a defined concentration is 0.43%, which corresponds to a BPA concentration of 4.38×10^{-11} M. Fig. 4b also shows the error bars corresponding to the range of electrical current measured for the three replicates at each concentration of BPA. The fact that the range of the error bars in Fig. 4b is so small is probably due to the fact the measurements are made in dry conditions. The CNTFET is able to detect concentrations of BPA at the picomolar range well below the legal limits and also below the limits of detection obtained in previous methods for analyzing BPA. The decrease in the electrical current in Fig. 4a after the addition of the different concentrations of BPA can be attributed to different reasons: (i) a charge transfer produced by the molecular recognition process between ER-α and BPA, probably through hydrogen bonding between the phenolic group of the BPA and the binding site in ER-α, as well as the hydrophobic and steric properties of BPA. (Rich et al., 2002) This recognition event may induce a steric modification of the adsorbed ER-α, increasing the charge transfer from the nuclear receptor to the nanotubes; (ii) the Schottky barrier modulation effect produced by molecules adsorbed very near to the metal-SWCNT contacts. Since

BPA is a much smaller molecule than ER-α, we do not think that in this case the main mechanism can be attributed to a scattering potential generated by the interaction between BPA and ER-α. We also do not think that the main mechanism is a decrease in the carrier mobility because Heller et al. (Heller et al., 2008) claim that this mechanism is unlikely to dominate sensing.

The selectivity of the CNTFETs was checked by measuring other pollutants that can be found together with BPA and which therefore can behave as interferences. The tested compounds are fluoranthene, pentacloronitrobenzene and malathion. These compounds were selected because they have been found, like BPA, in water samples. They are also highly toxic and are widely used as pesticides, fungicides and acaricides. Fig. 5 shows the electrical curve of the functionalized CNTFET device after the addition of different concentrations of fluoranthene. These results were similar with pentachloronitrobenzene and malathion (see supplemental information). We can see in Fig. 5 that even concentrations of 10^{-5} M of the interference do not change the electrical current with respect to the response generated by the functionalized CNTFET (the PBSTG curves in Fig. 5a). We have also carried out the detection of increasing BPA concentrations ($4.38x10^{-12}$ M, $4.38x10^{-9}$ M, $4.38x10^{-6}$ M and $4.38x10^{-5}$ M) in the presence of fluoranthene ($4.95x10^{-6}$ M). The electrical behaviour shown in Fig. 4 was observed showing that determination of BPA in presence of high concentration of interferences is possible.

To check the stability of the functionalized CNTFETs, some functionalized CNTFET devices were stored at room temperature and other ones at 8ºC. Every 24 hours the CNTFET devices were exposed for 2 min to increasing BPA concentrations ($4.38x10^{-12}$ M, $4.38x10^{-9}$ M, $4.38x10^{-6}$ M and $4.38x10^{-5}$ M) and the electrical responses were recorded. The electrical behaviour shown in Fig. 4 was observed the first four days only for the CNTFETs stored at room temperature. So the CNTFET devices are stable at least for four days stored at room temperature. We tried to regenerate the sensor by using several regeneration solutions (0.4 M glycine/HCl, pH 2.2, and 0.5 M NaCl). However, we were not able to fully recover the initial baseline again.

4. Conclusions

In this paper we have developed a fast and selective biosensor device for detecting BPA. It is based on using ER-α as a recognition layer adsorbed onto the nanotubes of our CNTFET device. For the first time a CNTFET has been functionalized with a

nuclear receptor, and we show that large molecules (i.e. ER-α) can be successfully used as the recognition layer for the ultrasensitive and selective detection of small molecules such as BPA. The concentrations of BPA detected with this device (pM) are smaller than any other detection method of BPA reported so far in the literature. The analysis time is also very short (2 minutes), which shows that this biosensor can be a useful label-free platform for detecting other small analytes by using an adequate nuclear receptor.

Acknowledgements

The authors would like to thank the Spanish Ministry of Science and Education (projects NAN2004-09306-C05-05 and CTQ2007-67570/BQU) and the European Union (project STRP 01071) for financial support. ZS also acknowledges the University of Pamplona and the Rovira i Virgili University for providing economic support. The authors would also like to thank Francesc Pérez and his research group in CNM/CSIC (Bellaterra, Spain) for providing the lithographic processes.

References

Bi, X., Wong, W.L., Ji, W., Agarwal, A., Balasubramanian, N., Yang, K.L., 2008. Biosens. Bioelectron. 23, 1442-1448.

Bradley, K., Briman, M., Star, A., Grüner, G., 2004. Nano Lett. 4, 253-256.

Byon, H.R., Choi, H.C., 2006. J. Am. Chem. Soc. 128, 2188-2189.

Cid, C.C., Riu, J., Maroto, A., Rius, F.X., 2008. Analyst. 133, 1005-1008.

Chen, R.J., Bangsaruntip, S., Drouvalakis, K.A., Wong Shi Kam, N., Shim, M., Li, Y.M., Kim, W., Utz, P.J., Dai, H., 2003. Proc. Natl. Acad. Sci. 100, 4984-4989.

Chen, R., Choi, H., Bangsaruntip, S., Yenilmez, E., Tang, X., Wang, Q., Chang, Y., Dai, H., 2004. J. Am. Chem. Soc. 126, 1563-156.

Gatidou, G., Thomaidis, N.S., Stasinakis, A.S., Lekkas, T.D., 2007. J. Chromatogr. A. 1138, 32-42.

Grüner, G., 2006. Anal. Bioanal. Chem. 384, 322-335.

Heller, I., Janssens, A.M., Männik, L., Minot, E.D., Lemay, S.G., Dekker, C., 2008. Nano Lett. 8, 591-595.

Hiroi, H., Tsutsumi, O., Momoeda, M., Takai, Y., Osuga, Y., Taketani, Y., 1999. Endocr. J. 46, 773-778.

Hu, L., Hecht, D.S., Grüner, G., 2004. Nano Lett. 4, 2513-2517.

Hu, Y., Zheng, Y., Zhu, F., Li, G., 2007. J. Chromatogr. A. 1148, 16-22.

Iijima, S., 1991. Nature. 354, 56-58.

Inoue, K., Yoshida, S., Nakayama, S., Ito, R., Okanouchi, N., Nakazawa, H., 2006. Arch. Environ. Contam. Toxicol. 51, 503-508.

Kauffman, D.R., Star, A., 2008. Chem. Soc. Rev. 37, 1197-1206.

Kawaguchi, M., Inoue, K., Yoshimura, M., Sakui, N., Okanouchi, N., Ito, R., Yoshimura, Y., Nakazawa, H., 2004. J. Chromatogr. A. 1041, 19-26.

Kim, W., Choi, H.C., Shim, M., Li, Y., Wang, D., Dai, H., 2002. Nano Lett. 7, 703-708.

Kim, S.N., Rusling, J.F., Papadimitrakopoulos, F., 2007. Adv. Mater. 19, 3214-3228.

Lin, C.H., Hsiao, C.Y., Hung, C.H., Lo, Y.R., Lee, C.C., Su, C.J., Lin, H.C., Ko, F.H., Huang, T.Y., Yang, Y.S., 2008. Chem. Commun. 5749-5751.

Maehashi, K., Katsura, T., Kerman, K., Takamura, Y., Matsumoto, K., Tamiya, E., 2007. Anal. Chem. 79, 782-787.

Moors, S., Blaszkewicz, M., Bolt, H.M., Degen, G.H., 2007. Mol. Nutr. Food. Res. 51, 787-798.

Mueller, S., 2004. Anal. Bioanal. Chem. 378, 582-587.

Oosterkamp, A., Hock, B., Seifert, M., Irth, H., 1997. Trends Anal. Chem. 16, 544– 553.

Peng, X., Wang, Z., Yang, C., Chen, F., Mai, B., 2006. J. Chromatogr. A. 1116, 51-56.

Piao, M.H., Noh, M.H., Rahman, M.A., Won, M.S., Shim, Y.B., 2008. Electroanalysis. 20, 30-37.

Rich, R.L., Hoth, L.R., Geoghegan, K.F., Brown, T.A., LeMotte, P.K., Simons, S.P. Hensley, P., Myszka, D.G., 2002. Proc. Natl. Acad. Sci. 99, 8562-8567.

Riu, J., Maroto, A., Rius, F.X., 2007. Talanta. 69, 288-301.

Rodriguez-Mozaz, S., Lopez de Alda, M., Barceló, D., 2005. Water Res. 39, 5071-5079.

Schwartz-Mittelman, A., Baruch, A., Neufeld, T., Buchner, V., Rishpon, J., 2005. Bioelectrochemistry. 65,149-156.

Shim, M., Wong Shi Kam, N., Chen, R.J., Li, Y.M., Dai, H., 2002. Nano Lett. 2, 285-288.

So, H.M., Park, D.W., Jeon, E.K., Kim, Y.H., Kim, B.S., Lee, C.K., Choi, S.Y., Kim, S.C., Chang, H., Lee, J.O., 2008. Small. 4, 197-201.

Star, A., Gabriel, J., Bradley, K., Grüner, G., 2003. Nano Lett. 3, 459-463.

Star, A., Joshi, V., Han, T.R., Altoé, M.V. P., Grüner, G., Stoddar, J.F., 2004. Org. Lett. 6, 2089-2092.

Star, A., Tu, E., Niemann, J., Gabriel J-C.P., Joiner, C.S., Valcke, C., 2006. Proc. Natl. Acad. Sci. 103, 921-926.

Villamizar, R.A., Maroto, A., Rius, F.X., Inza, I., Figueras, M.J., 2008. Biosens. Bioelectron. 24, 279-283.

Vom Saal, F.S., Akingbemi, B.T., Belcher, S.M., Birnbaum, L.S., Crain, D.A., Eriksen, M., Farabollini, F., Guillette, L.J., Hauser, R., Heindel, J.J., Ho, S.M., Hunt, P.A., Iguchi, T., Jobling, S., Kanno, J., Keri, R.A., Knudsen, K.E., Laufer, H., LeBlanc, G.A., Marcus, M., McLachlan, J.A., Myers, J.P., Nadal, A., Newbold, R.R., Olea, N., Prins, G.S., Richter, C.A., Rubin, B.S., Sonnenschein, C., Soto, A.M., Talsness, C.E., Vandenbergh, J.G., Vandenberg, L.N., Walser-Kuntz, D.R., Watson, C.S., Welshons, W.V., Wetherill, Y., Zoeller, R.T., 2007. Reprod. Toxicol. 24, 131-138.

Walsh, D.E., Dockery, P., Doolan, C.M., 2005. Mol. Cell. Endocrinol. 230, 23–30.

Wozniak, A.L., Bulayeva, N.N., Watson, C.S., 2005. Environ. Health. Perspect. 113, 431–9.

Zhao, Y.L., Hu, L.B., Stoddart, J.F., Grüner, G., 2008. Adv. Mater. 20, 1910-1915.

Zsarnovszky, A., Le, H.H., Wang, H.S., Belcher, S.M., 2005. Endocrinology. 146, 5388–5396.

Figure captions

Fig. 1: Functionalization process of the SWCNTs; (a) scheme of a SWCNTs network; (b) adsorption of ER-α onto the SWCNTs network; (c) the gaps left on the SWCNTs after the adsorption of the ER-α are covered by a PBSTG blocking solution (0.05% Tween 20 and 0.8% gelatin in PBS).

Fig.2: ESEM image of the source and drain electrodes and of the network of SWCNTs.

Fig.3: Electrical characterization. Source–drain current (I) *vs.* gate voltage (Vg) of a typical CNTFET after each functionalization step: as-grown nanotubes (), ER-α (), PBSTG ( ) and 2.19×10^{-12} M of BPA (). Vsd = 0.25 V.

Fig. 4: Electrical characteristics of the CNTFET. Fig. 4a: Gate voltage (Vg) dependence of the source-drain current (I) of a typical functionalized CNTFET before exposure to BPA ( ) and after exposure to different solutions from 2.19×10^{-12} M () up to 4.38×10^{-4} M () of BPA. Each electrical curve corresponds to the mean value of three replicates. Vsd = 0.25 V. Fig. 4b: Behaviour of the source-drain current vs. increasing BPA concentrations (M) at Vg=- 5V.

Fig. 5: Electric response of the CNTFET in the presence of fluoranthene. Vsd = 0.25 V. The baseline corresponding to the functionalized CNTFET is the ( ) PBSTG curve. The inset shows the behaviour of the source-drain current vs. increasing fluoranthene concentrations (M) at Vg=- 5V.

Figure 1

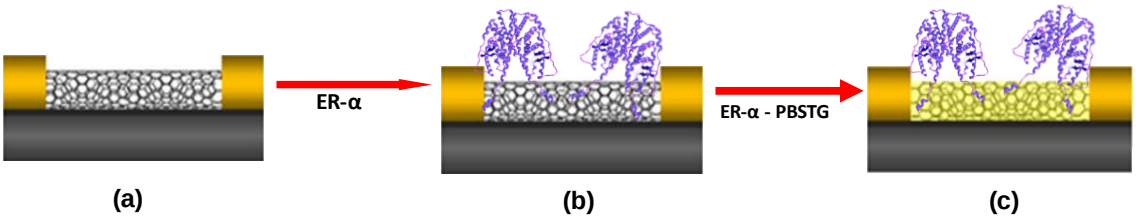

(a) (b) (c)

Figure 2

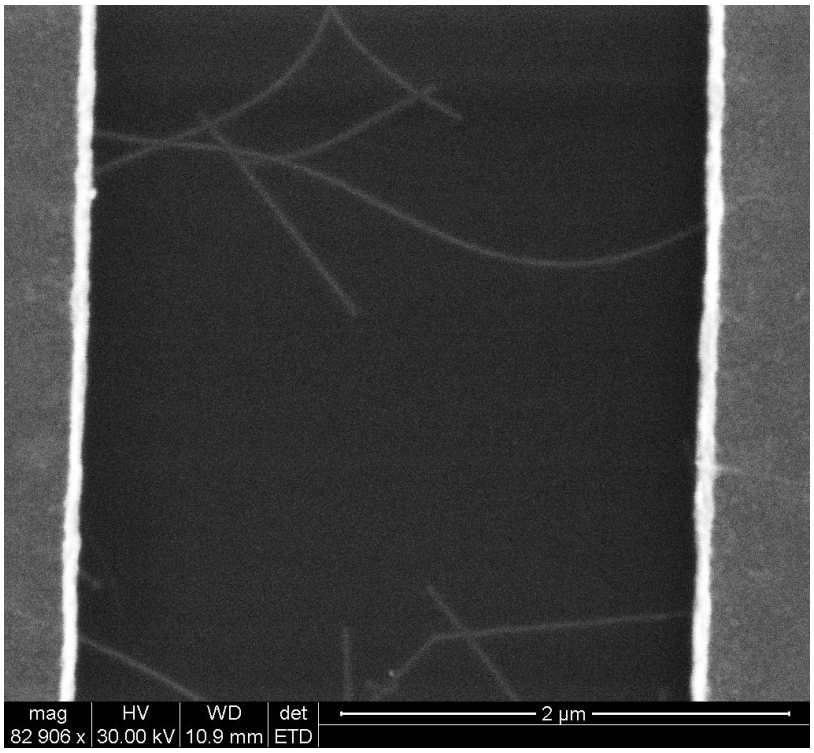

Figure 3

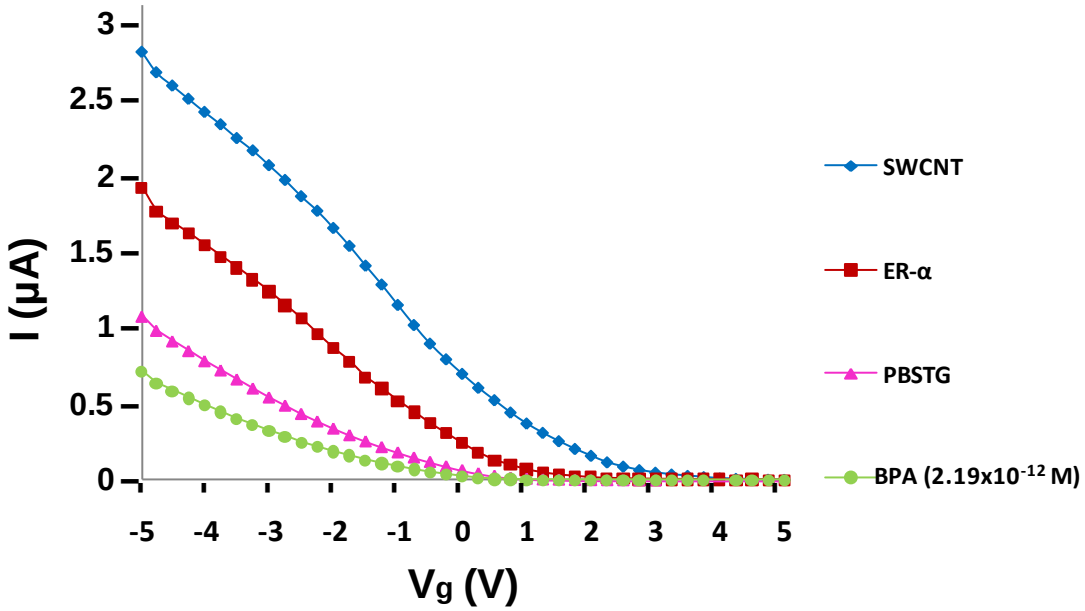
3
2.5
2
1.5
1
0.5
0
I (μA)
-5
-4
-3
-2
-1
0
1
2
3
4
5
Vg (V)
SWCNT
ER-α
PBSTG
BPA (2.19x10-12 M)

Figure 4

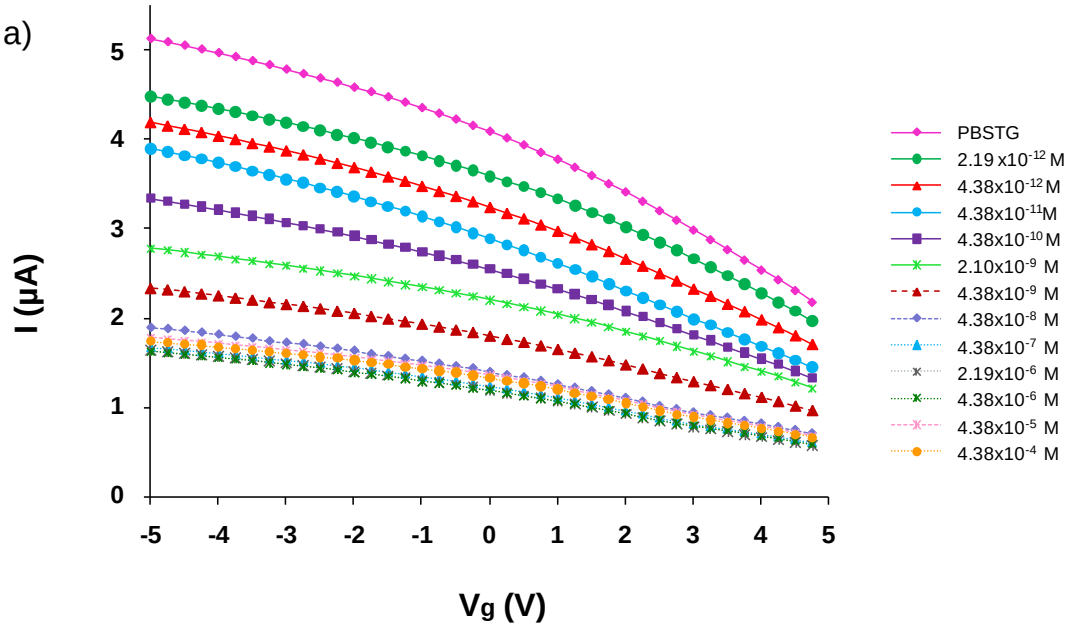
a)
I (µA)
Vg (V)
PBSTG
2.19 x10-12 M
4.38x10-12 M
4.38x10-11M
4.38x10-10 M
2.10x10-9 M
4.38x10-9 M
4.38x10-8 M
4.38x10-7 M
2.19x10-6 M
4.38x10-6 M
4.38x10-5 M
4.38x10-4 M

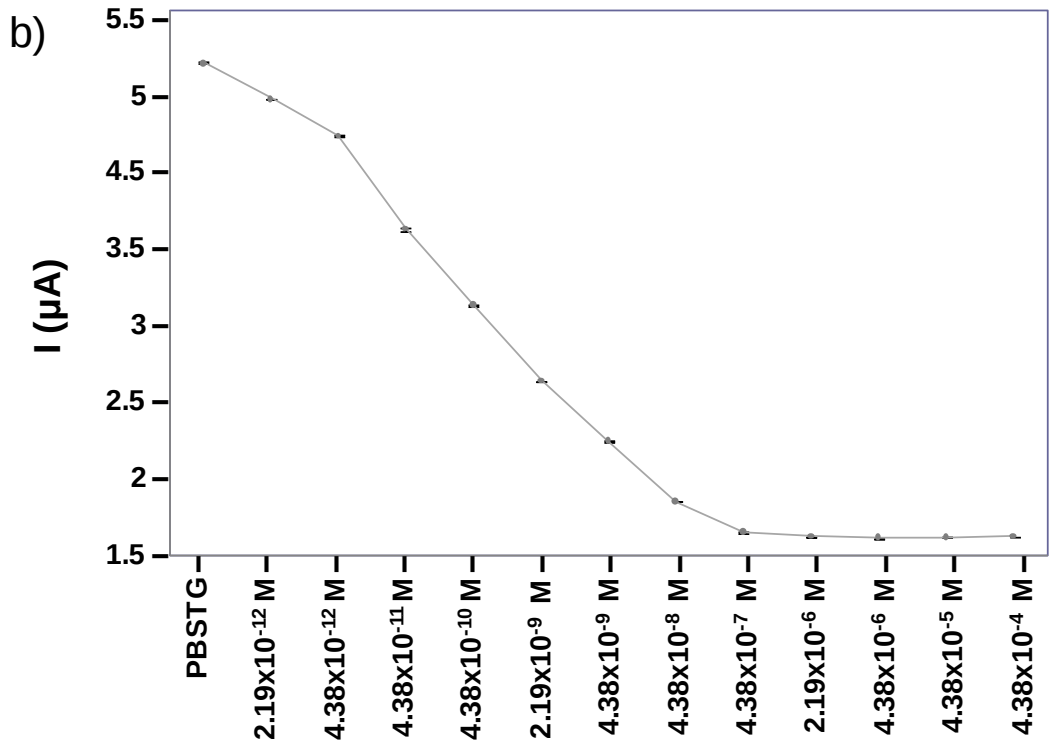
b)
I (µA)
PBSTG
2.19x10-12 M
4.38x10-12 M
4.38x10-11 M
4.38x10-10 M
2.19x10-9 M
4.38x10-9 M
4.38x10-8 M
4.38x10-7 M
2.19x10-6 M
4.38x10-6 M
4.38x10-5 M
4.38x10-4 M

Figure 5

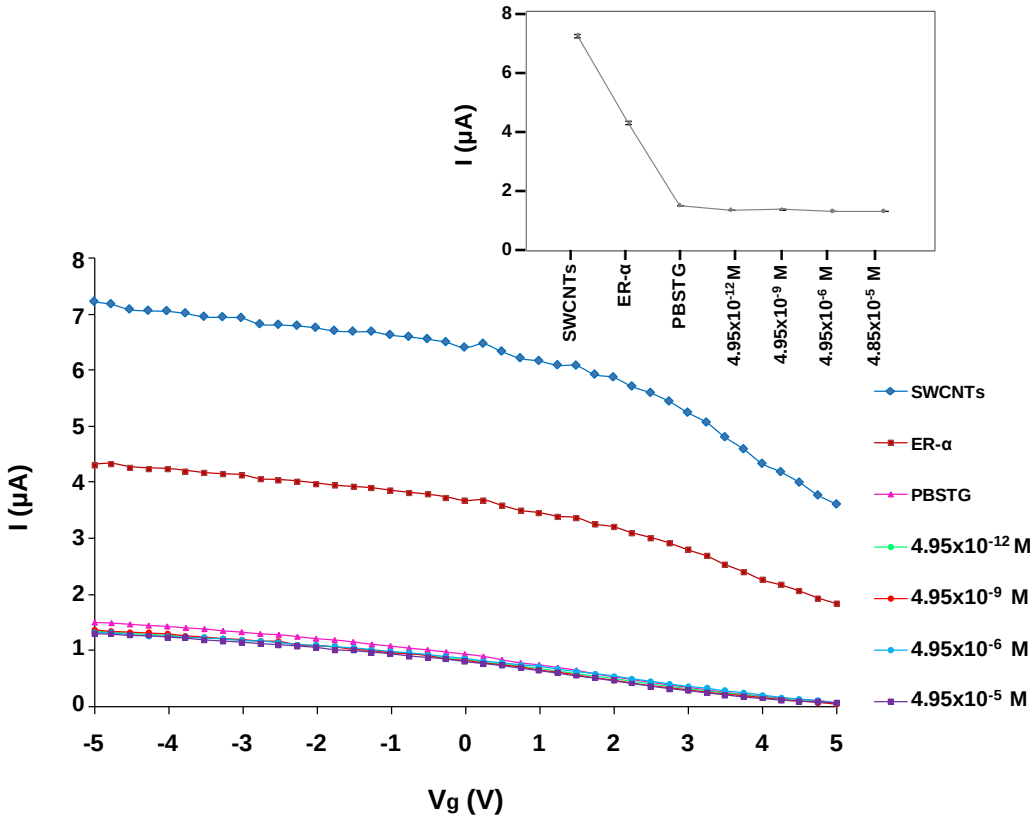
I (μA)
Vg (V)
SWCNTs
ER-α
PBSTG
4.95x10-12 M
4.95x10-9 M
4.95x10-6 M
4.85x10-5 M